Exergy and Energy Analysis of Wind-Thermal System

Nima Norouzi[*]

Department of Energy Engineering and Physics, Amirkabir University of Technology (Tehran Polytechnic), 424 Hafez Avenue, PO Box 15875-4413, Tehran, Iran

Current wind systems are intermittent and cannot be used as the baseload energy source. The research on the concept of wind power using direct thermal energy conversion and thermal energy storage, called wind powered Thermal Energy System (WTES), opened the door to a new energy system called Wind-thermal, which is a strategy for developing baseload wind power systems. The thermal energy is generated from the rotating energy directly at the top of the tower by the heat generator, which is a simple and light electric brake. The rest of the system is the same as the tower type concentrated solar power (CSP). This paper's results suggest that the energy and exergy performance of the WTES (62.5% and 29.8%) is comparable to that of conventional wind power, which must be supported by the backup thermal plants and grid enhancement. This cogeneration nature of the WTES system makes this system suitable for using wind power as a direct heat source in several heat-demanding processes such as chemical production. Also, the light heat generator reduces some issues of wind power, such as noise and vibration, which are two main bottlenecks of the wind power technology.

Introduction

Due to the industrialization of most cities, energy demand grew significantly. The continuous increase in energy demand has led to the widespread use of carbon-containing fossil fuels, which has caused significant damage to the environment and human health. In recent years, many efforts and programs have been made to reduce the use of fossil fuels. Renewable energy sources such as solar and wind energy have been introduced as reliable sources for clean energy production for use. Solar power plant technology using parabolic-linear concentrators is the most significant method among thermal-electric methods for renewable energy production.

Recently, Gupta *et al.* [1] proposed a system consisting of an organic Rankin cycle with a triple pressure level absorption system and a parabolic-linear solar collector system in 2020. This system generates electricity and refrigeration simultaneously at two different temperatures. In this study, the effect of different inlet parameters such as solar radiation, turbine inlet pressure, turbine outlet pressure, and evaporator temperature on the designed schematic subsystems was investigated. Kerme *et al.* [2] thermodynamically analyzed a multiple power generation system using the thermal energy from a solar system with a parabolic-linear solar collector. The results showed that increasing the turbine inlet temperature increased the efficiency and decreased overall energy losses.

The results also showed that the two main sources of exergy losses are the solar system and the desalination unit.

Alirahmi *et al.* [3] proposed a multiple generation system based on the geothermal energy and a parabolic-linear solar collector system for simultaneous electricity generation, cooling load, freshwater, hydrogen, and heat. To optimize the objectives of their research, EES (engineering equation solver) and MATLAB software were interconnected using the Dynamic Exchange Data method. Finally, the system exergy efficiency and total unit cost were 29.95% and 129.7 $/GJ, respectively. Alotaibi *et al.* [4] investigated the performance of a conventional steam power plant with a regenerative system equipped with a parabolic-linear solar collector system. The system analysis results showed that the removal of the low-pressure (LP) turbine increases the performance of the steam power plant up to 9.8 MW/h. The optimal area for the solar system in these conditions was estimated at 25,850 square meters. Ehyaei *et al.* [5] conducted thermodynamic analysis, energy and exergy, and economic analysis on a linear parabolic solar collector. The optimization results showed that the exergy efficiency, energy efficiency, and costs were 29.29%, 35.55%, and $0.0142/kWh, respectively. Toghyani *et al.* [6] used a nanofluid as a cooling fluid in a parabolic-linear solar collector to cool the solar system and produce hydrogen. The results showed that hydrogen production increases under higher solar intensities because the Rankin cycle transfers more energy to the PEM.

AlZahrani and Dincer [7], in 2018, studied the energy and exergy of parabolic-linear solar collectors as part of a solar power plant under different design and performance conditions. Finally, the energy and exergy efficiency rates of 35.66% and 38.55% were reported, respectively. In 2019, Yilmaz [8] reviewed the comprehensive thermodynamic performance and economic evaluation of a combined ocean thermal energy system and a wind farm. The results showed that the hybrid system's overall energy and exergy efficiencies are 12.27% and 34.34%, respectively. The cost of the proposed system was reported to be $3.03 per hour. Ishaq and Dincer [9] proposed a new idea for hydrogen production from methanol using the wind energy. The proposed system used industrial carbon emissions to produce methanol. EES and Aspen Plus software was used to model the system and comprehensively analyze it. Bamisile *et al.* [10] modeled a power generation system using wind, solar and biogas energy, and analyzed the energy and exergy of the system. The results showed that the system's overall energy efficiency varies from 64.91% to 71.06%, while the exergoconomic efficiency increases from 31.80% to 53.81%. In 2018, Kianfard *et al.* [11] investigated a renewable system based on thermal energy to produce fresh water and hydrogen. The economic analysis results showed that the investment costs per unit of reverse osmosis desalination plant were 56%. The cost of producing freshwater was estimated at 32.73 cents per cubic meter.

Alirahmi and Assareh [12] analyzed the energy, exergy, and economy and multi-objective optimization of multiple energy systems, including hydrogen production, freshwater, cooling, heating, hot water, and electricity generation of Dezful city. The two objective functions of this study were exergy and total cost, which were optimized by a genetic algorithm. Finally, the best value for the exergy efficiency was 31.66%, and the total unit rate was 21.9 $/GJ. In 2020, Mohammadi *et al.* [13] designed a combined cycle gas turbine to generate electricity, freshwater, and cooling. The results showed that the use of reverse osmosis is more economical than a combined multi effect distillation and reverse osmosis (MED-RO) system. System costs for electricity, water, and cooling were

also reported at $ 0.0648 per kilowatt-hour, $ 0.7219 per cubic meter, and $ 0.0402 per hour, respectively.

In the aforementioned studies, there is no numerical modeling for wind turbines. It is often assumed that the wind turbine is working under a steady operation condition, and the effect of the changing parameters of the wind turbine on the system was not studied.

In this study, a numerical modeling method is used to model a horizontal axis wind turbine coupled with a direct heat generator and a phase change material (PCM) storage to enhance baseload reliability of the wind system, including an organic Rankine cycle (ORC), a wind turbine, and a PCM storage. The model studied the effects of the different wind turbine's operation conditions on the performance of the described system based on the energy and exergy efficiencies (2E analysis), and finally evaluated the operating conditions for the best overall technical performance of the system.

Materials and Methods

Case Study

The installation of renewable energy sources in the electricity grid creates many problems, because most renewables are intermittent [14]. This article describes a new idea called Wind Thermal Power (WTES), which was first proposed to solve network problems.

Concentrated Solar Power (CSP) is attracting attention due to its susceptibility to scattering. Some plants can operate with continuous power generation 24 hours a day. Thermal energy storage has already become the second-largest energy storage system in the United States after hydrogen. Solana, which has been online since 2013, has a massive 1,680 megawatt-hour power reserve. Total thermal energy storage will almost double in 2015 [3]. Proposals using this practical thermal energy storage are gradually increasing [4-6]. The use of energy storage is also studied from various aspects [7, 8].
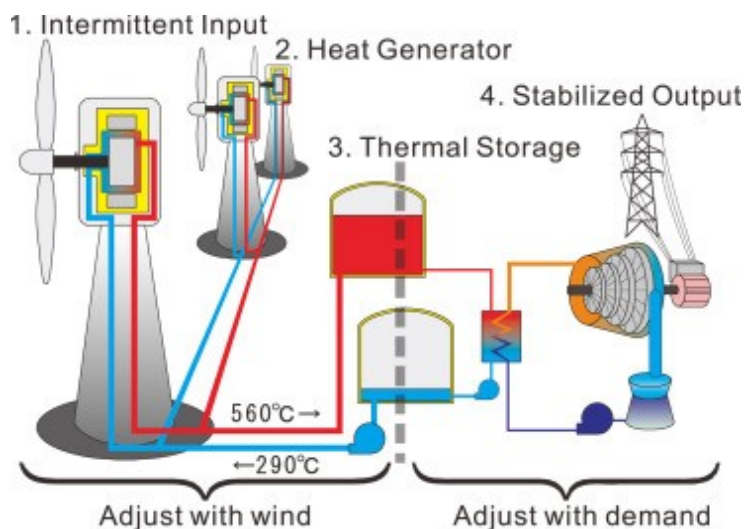

Fig. 1. Schematic of the system

The use of this thermal energy storage and a low-cost and lightweight heat generator are key points of WTES. A typical shape of a "specialized thermal type" WTES is shown in Fig. 1. The rotational energy is converted into thermal energy just above the tower. The rest of the system is of the same type as the CSP turret [9]. The thermal energy generated is transferred to the base facilities by means of a heat transfer fluid (HTF) and produces steam to power the turbine generator when required.

This system is sub-divided into three subsystems and studied in the term of exergy and energy. The mentioned subsystems are wind turbine, storage system, and wind turbine system.

Wind Turbine Energy Analysis

If we consider a wind turbine consisting of three general parts of blades, mechanical equipment, and generator (as shown in Fig. 2), then to analyze the power in each part, energy analysis must be used. The result of using energy analysis is the following Eqs 1 to 4 for turbine power [13].

$$p_w = \frac{1}{2}\rho A v^3 \tag{1}$$

$$p_m = p_w \eta_b \tag{2}$$

$$p_G = p_m \eta_m \tag{3}$$

$$Q_G = p_G \eta_g = \frac{1}{2}\rho A V^3 \eta_m \eta_G \eta_b \tag{4}$$

In the above equations, η_b stands for blade efficiency, η_m is mechanical efficiency of turbine, η_g is generator's efficiency, V is wind speed, A is effective area of wind turbine, ρ is air density, Q_G is turbine output heat, p_G is power received by the generator, p_m is power received by mechanical parts, and p_w is maximum power of the wind[14].
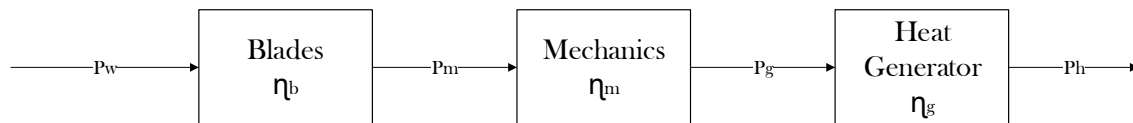

Fig. 2. Schematic of the general parts of a wind turbine

Wind Turbine Exergy Analysis

The exhaust air outlet of the turbine is shown in Eq. (5):

$$EX_{air} = EX_{kinetic} + EX_{potential} + EX_{ph} + EX_{ch} \tag{5}$$

where EX symbolizes the exergy in the above relation, and the substrates of each symbol represent the relevant part (kinetic, potential, physical, and chemical). If we consider the environment as 298 K and air at 1 atm pressure, the chemical and physical exergy of the air will be zero. Because the height of the air does not change, the potential exergy will be zero. So, the air exergy is calculated from $EX_{air} = EX_{kinetic}$, and mass flow and airflow exergy are obtained from the following Eqs 6 and 7 [15]:

$$m = \rho A V_r = \rho \pi R^2 V_r \tag{6}$$

$$EX_{kinetic} = \frac{V_r^2}{2} \tag{7}$$

where M, R, and V_r are equal to mass flow, rotor radius, and wind speed at high relationships, respectively. If we consider the turbine in the simplified form of Fig. 3, in this figure, the wind turbine consists of blades (which are assumed to be without friction), mechanical equipment (including shaft, bearing, and gearbox with ηm efficiency) and

heat generator with η_G efficiency is considered. As can be seen from the figure, the energies in the flow are in the form of kinetic, work-oriented, and electrical forms that can be fully converted to work, *i.e.*, the current exergy is equal to the content of the flow energy. If for analysis, we consider the system only as a turbine set, then the feed exergy of the system is equal to the state 1 exergy flow and the product exergy flow is equal to the exergy flow of the state 2. The flows are marked with a number on the figure. The exergy of the flows will be in the form of the following Eqs 7 to 12 [16]:

$$EX_1 = m\left(\frac{V_{in}^2}{2}\right) \tag{7}$$

$$EX_2 = m\left(\frac{V_{out}^2}{2}\right) \tag{8}$$

$$EX_3 = EX_1 - EX_2 \tag{9}$$

$$EX_4 = \eta_m EX_3 \tag{10}$$

$$EX_5 = constant\ in\ let\ water \sim 0 \tag{11}$$

$$EX_6 = \eta_G EX_5\left(1 - \frac{T_5}{T_6}\right) \tag{12}$$

In the above equations, EX represents the flow of exergy (multiplied by mass flow), and V_{in} and V_{out} are equal to the velocity of the inlet and outlet winds, respectively.
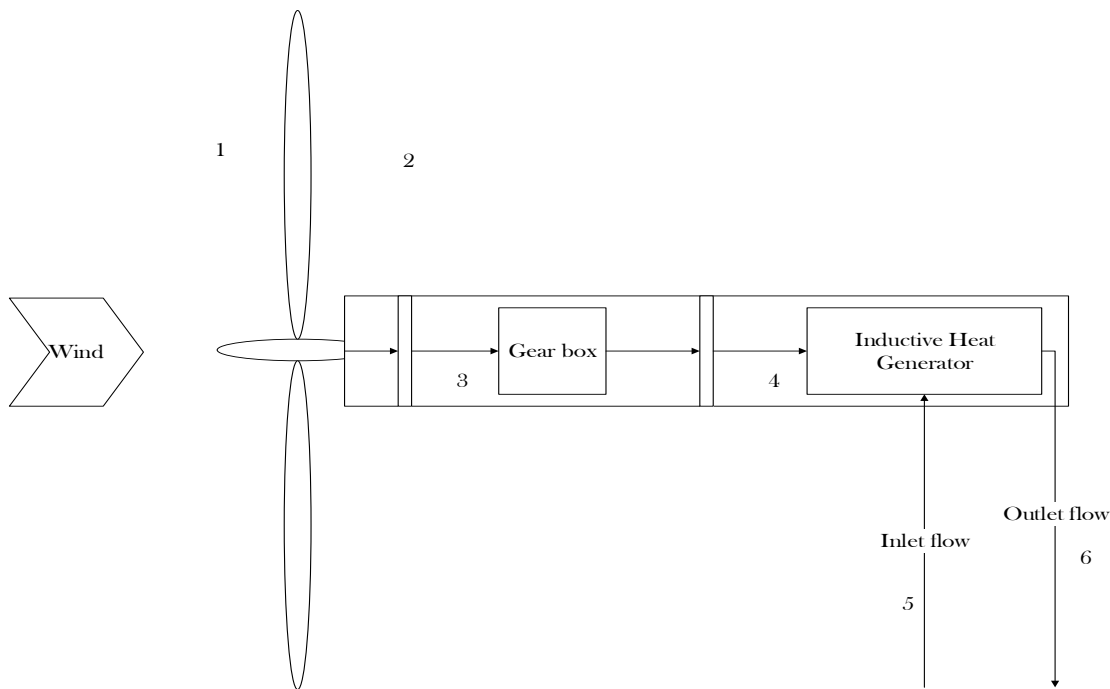

Fig. 3. Schematic of a wind turbine with a display of exergy flows in the turbine assembly

In a wind turbine, the part of the input wind power that is out of the turbine's reach is called the exergy loss and will be equal to the flow exergy of state 1. Also, the part of the exergy, which is lost in the equipment and different parts of the conversion turbine due to friction and inefficiencies of that component and turns into other forms of energy (such as heat), is called exergy destruction which is equal to the difference in exergy level between inlet and output flow (as defined by Eq. (13) [17]):

$$EX_D = EX_{in} - EX_{out} \tag{13}$$

In the above relation, EX_{in}, EX_{out}, and EX_D are equal to the output current exergy, the input current exergy, and the exergy degradation, respectively. Therefore, the

degradation of the exergies of different parts in a turbine can be calculated from Eqs 14 to 16:

$$EX_D = EX_3 - EX_4 = EX_3 - \eta_m EX_3 = EX_3(1 - \eta_m) \tag{14}$$

$$EX_{DG} = EX_4 - EX_6 = \eta_m EX_3 - \eta_G EX_4 = \eta_m EX_3 - \eta_G \eta_m \left(1 - \frac{T_5}{T_6}\right) EX_3 \tag{15}$$

$$EX_{DG} = EX_3 \eta_m \left(1 - \eta_G \left(1 - \frac{T_5}{T_6}\right)\right) \tag{16}$$

where EX_D, EX_{DG} and EX_D are the total exergy damage, the generator exergy degradation, and the exergy degradation of the mechanical part, respectively. For each part, a quantity called the degradation ratio is defined, which is equal to the degradation ratio of that part to the system feed exergy. It is defined in Eqs 17 to 20 [18]:

$$y_{D,t} = \frac{E_{D,t}}{E_f} \tag{17}$$

$$y_{D,G} = \frac{E_{D,G}}{E_f} \tag{18}$$

$$y_{D,m} = \frac{E_{D,m}}{E_f} \tag{19}$$

$$y_{D,tot} = \frac{E_{D,tot}}{E_f} \tag{20}$$

where $y_{D,t}$ is equal to the degradation ratio in the t part and t can be equal to G, m and tot, which represent the generator, the mechanical part and the whole system, respectively. Also, the exergy efficiency of the whole turbine system is defined as the ratio between the output current exergy to the feed flow exergy as calculated in Eq. (21):

$$exergy\ efficiency_{sys} = \frac{e_p}{e_f} = \frac{EX_6}{EX_1} = \frac{\eta_G \eta_m \left(1 - \frac{T_5}{T_6}\right)}{EX_1} \tag{21}$$

Replacing the new system requires an analysis of many different aspects. Therefore, in the first step of designing the power generation system, the desired system should be adapted to thermodynamics' rules and principles. Due to the CHP system's combination with two different types of generators as the prime movers, energy analysis must be performed. The purpose of these calculations is to determine the best type of combination with the highest output power, recycled heat, overall efficiency, and the lowest fuel consumption of the system.

Storage Exergy Analysis
Having some practical considerations, a commercial PCM melting point of which is 250 °C (PlusICE H250) is used as a case study. The supplied exergy by HTF during the charging period, the output exergy at discharging cycle, and the exergetic efficiency of PCM storage can be expressed by the following equations, where T_0, T_6, T_7, and T_m refer to temperatures of ambient, HTF inlet, HTF outlet, and PCM melting point, respectively. Storage heat-loss is considered to be negligible [19]:
Charging is calculated in Eq. (22):

$$EX_{pcm.i} = \dot{m}_{HTF}\ C_{HTF}[(T_6 - T_7) - T_0 \ln(T_6/T_7)] \tag{22}$$

Discharging is calculated in Eq. (23):

$$EX_{pcm.o} = \dot{m}_{HTF} \, C_{HTF}[(T_7 - T_6) - T_0 \ln(T_7/T_6)] \tag{23}$$

Charge and Discharge are calculated in Eq. (24):

$$T_7 = T_m + (T_7 - T_m)e^{-(h_{pcm}A_{pcm}/\dot{m}_{pcm}C_{pcm})} \tag{24}$$

Exergetic PCM storage efficiency is calculated in Eq. (25):

$$\eta_{pcm} = EX_{pcm.o}/EX_{pcm.i} \tag{25}$$

where $\dot{m}_{HTF} = 6.2 \, (kg/s)$. Also, it is assumed that the isothermal PCM melts, and the sensible heat of the PCM is negligible. Moreover, to minimize any unsatisfactory conditions, it is considered that the controlling system would block the storage tank's path as soon as the difference between T_7 and T_m falls below 30°C. The total exergetic outcome of the system with PCM storage is determined as shown in Eq. (26):

Total output exergy= $EX_u + EX_{pcm.o}$ (26)

Finally, the overall exergetic efficiency of the whole system is measured by dividing the sum of all output exergy by the amount of input exergy of the solar system.

Results showed that using "*PlusICE H250*" as the latent heat storage (LHS) for the Shiraz power plant is suitable due to both PCM physical properties and power plant working conditions, such as HTF temperature (see Table 1)[20].

Table 1. Selected LHS with PlusICE H250 exergetic analysis results

Parameter	unit	value
Exergetic efficiency	(%)	85.54
Exergy Loss	(W)	30200
$EX_{pcm.o}$	(W)	103448
$EX_{pcm.i}$	(W)	133567
Density	(kg/m^3)	2380
Latent heat	(kJ/kg)	280
Specific heat	(kJ/kg K)	1.525
Max working temperature	(°C)	600
Melting point	(°C)	250
Material		PlusICE H250

Rankin cycle

The heat given to the ORC heat exchanger can be calculated by balancing the energy between the operating fluid and the wind tower fluid at the heat exchanger inlet and outlet obtained from Eq. (27) (see Fig. 4).

$$\dot{Q}_6 = \dot{m}_{turbine}(h_7 - h_5) = \dot{m}_{ORC}(h_8 - h_{11}) \tag{27}$$

where $\dot{m}_{turbine}$ is the mass flow rate of geothermal water, and $\dot{m}_{ORC}$ is the mass flow rate of the ORC cycle. By applying the energy balance, the production capacity of the turbine is obtained from Eq. (28).

$$\dot{W}_t = \dot{W}_{t,isen} \, \eta_t = \eta_t \, \dot{m}_{ORC} \, ((h_8 - h_9)) \tag{28}$$
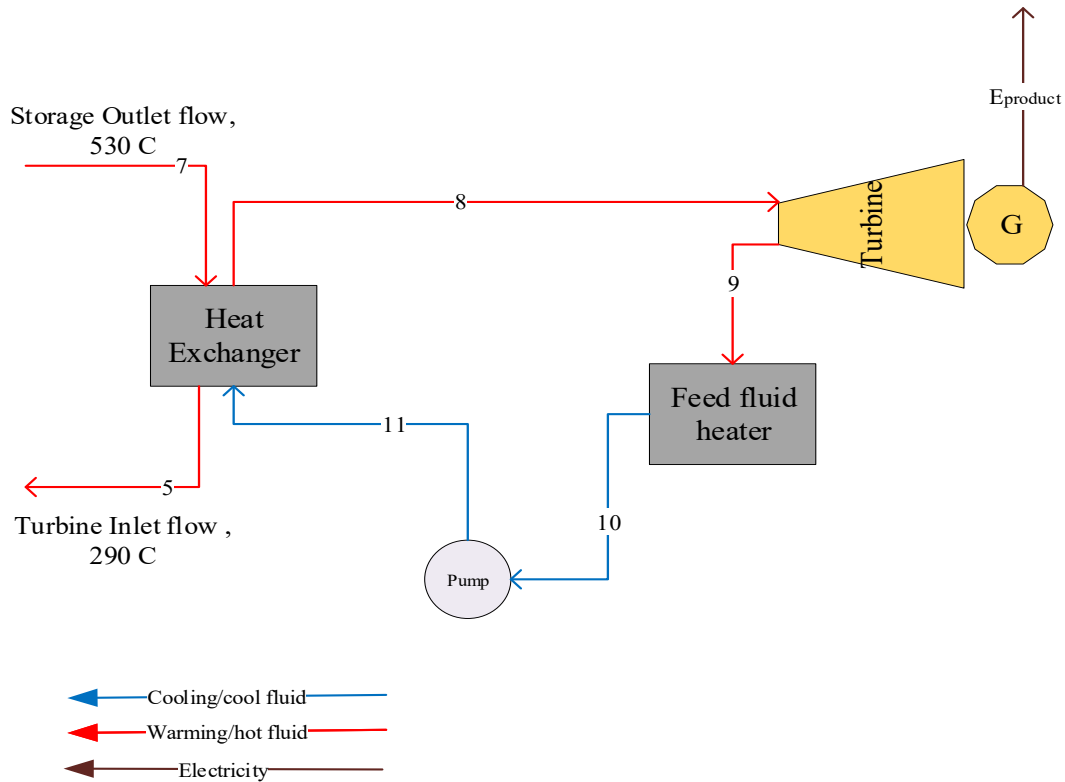
Fig. 4. Schematic of a Rankine system used in the wind turbine system

The heat given to the cooling water in the condenser is calculated from Eq. (29).

$$\dot{Q}_C = \dot{m}_{ORC} (h_{10} - h_9) \tag{29}$$

The consumption of pumps in the cycle is calculated from Eq. (30).

$$\dot{W}_P = \dot{W}_{P1} = \frac{\dot{m}_{ORC}}{\eta_P} (h_{11} - h_{10}) \tag{30}$$

The net generated power of the ORC cycle is obtained from the algebraic sum of the turbine-generated power and the pump consumption, which is injected into the grid directly as $E_{product}$ calculated in Eq. (31).

$$\dot{W}_{net} = \dot{W}_t - \dot{W}_P = \dot{E}_{Product} \tag{31}$$

The energy efficiency of the Rankin cycle is calculated from Eq. (32)[21].

$$\eta_{ORC} = \frac{\dot{W}_{net}}{\dot{Q}_{HX}} \tag{32}$$

Results and Discussion

Validation

In this section, before presenting the results, the values and results obtained are first validated. The purpose of accreditation is to ensure the simulation and its results.

Implementing the 2E method can allow us to make satisfactory predictions about the energy produced under different conditions and calculate the wind speed behind the wind turbines to measure the energy and energy efficiency.

Figure 5 shows the comparison between the real-state power measurement and the power calculated by the 2E code. As shown in Figure 5, the 2E code has a good ability to predict the power output. Increasing the wind speed from 4 m/s to 15 m/s results in a

higher power output at all three tilt angles, whereas after reaching a peak at wind speeds of 11.5 m/s, it has an opposite effect on the power output. On the other hand, increasing the bank angle decreases the power output at all wind speeds. This reduction makes more sense at higher wind speeds. Wind turbines are expected to have the highest performance at a wind speed of 12 m/s and a tilt angle of 5 degrees, producing a power of 140 kW.
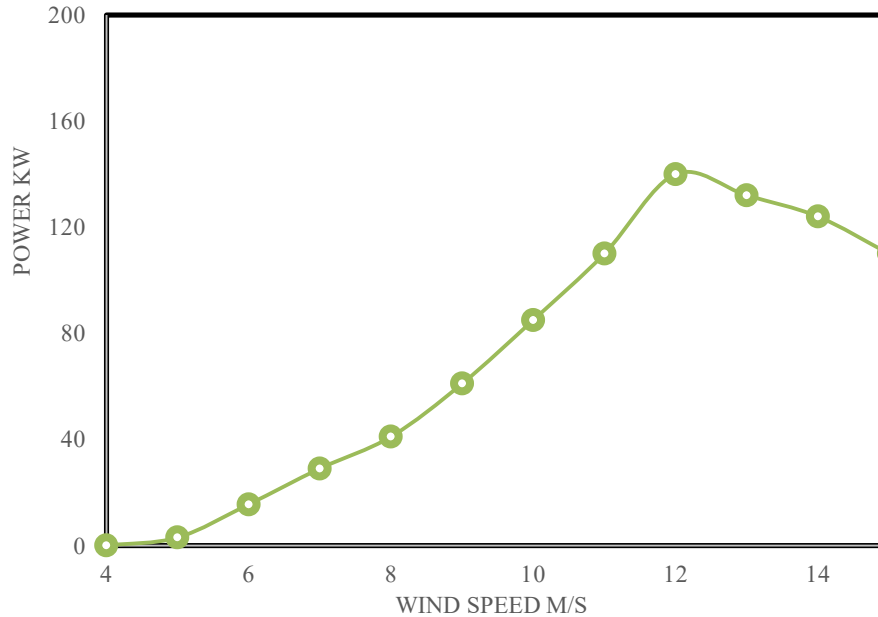

Fig. 5. Comparison of output power between BEM model and experimental data

Wind Turbine's Energy and Exergy Analyses

As seen in Table 2, the wind speed significantly affects the wind turbine's performance based on energy and exergy efficiencies. It causes a steady rise in exergy flow and destruction. The maximum exergy and energy efficiencies are 44.9 % and 46.7 % at wind speed 11.5 m/s, respectively.

Table 2. 2E analysis for wind system in different wind speeds

Wind speed (m/s)	Energy efficiency (%)	Exergy efficiency (%)	Exergy flow (W)	Exergy destruction (W)
6	15.1	13.8	55833.8	12037.2
7	34.7	31.5	86571.5	18203.9
8	43.8	41.6	127209.6	24587.9
9	44.8	43.1	179150	33692.4
10	46.8	45.2	243812.1	44596.7
11	45.7	44.4	322612.5	56701.1
12	46.7	44.9	416960.3	71283.5
13	32.8	32.1	528321.2	74462.9
14	25	24.6	658063.4	75354.3
15	18.3	18	807607.5	71847.3

Table 3 shows that increasing the pressure change can decrease the wind turbine exergy efficiency while increasing the temperature can increase the exergy efficiency from 42.1% at 5°C to 43% at 35°C. However, these changes are not noticeable from the velocity's affect on the wind turbine's exergy efficiency.

Table 3. The effect of pressure changes and temperature on the exergy efficiency of wind turbine

Variables	Exergy efficiency (%)
P= 100 Kpa	44.9
P= 150 Kpa	44.7
P= 200 Kpa	44.6
P= 250 Kpa	44.2
T= 5°C	44.5
T= 20°C	44.7
T= 25°C	44.9
T=35°C	45.2

Results of the System

By comparing the references and the present work presented in Table 4, it can be seen that there is a good accuracy for the results of the calculated parameters in the present work.

Table 4. Performance parameters of organic Rankine cycle with feed fluid recovery and heating

Parameter	value
Fluid agent	R236fa
Heat Exchanger load (kW)	112
Condenser load (kW)	34.9
Turbine output power (kW)	77.0
Pump power consumption (kW)	2.9
Net power output (kW)	69.9
Energy efficiency (%)	62.4
Mass flow rate of operating fluid (kg/s)	1.1

Table 5 shows the performance characteristics of the system. All these values are calculated for four different operating fluids. It is observed that the operating fluid R245fa has the highest energy and exergy efficiency with 49.8% and 27.8%, respectively. Operating fluids R114, R600 and R236fa are also in the next categories in terms of performance characteristics. Table 5 shows the lost exergy rate of system components for all operating fluids. Examining the system's exergy based on the above tables shows that the exchanger and the inductive generator have the highest exergy destruction (heat degradation), because both fuels' exergy flow rate and temperature differences are very high. It is also observed that with the change of operating fluid, the exergy loss in the exchanger decreases. This trend is to increase the power by reducing the loss of exergy in the exchanger. Comparing the operating fluids exegetically, it is observed that the operating fluid R245fa has the lowest exergy loss and the operating fluid R236fa has the highest exergy loss in the exchanger. Therefore, it can be concluded that the operating fluid that has less exergy loss in the exchanger produces more power and produces higher exergy loss in the wind turbine (see Table 6).

Table 5. System performance characteristics

Performance characteristic	R236fa	R600	R114	R245fa
Direct power to grid (kW)	69.9	69.9	69.9	69.9
exchanger heat (kW)	112	112	112	112
Condensing heat (kW)	36.99	36.52	34.93	35.56
Turbine power (kW)	75.01	75.48	77.07	76.44
Pump power (kW)	5.11	5.58	7.17	6.54
Total thermal efficiency (%)	67.0	67.4	68.8	68.3
Rankine cycle exergy efficiency (%)	63.7	64	65.4	64.9
Exergy efficiency with wind system (%)	28.7	28.8	29.4	29.2

Table 6. Loss of exergy rate of different system components

System components	R236fa	R600	R114	R245fa
Pump	5.21	5.66	7.33	6.54
Storage	12.76	13.21	13.44	13.51
Turbine	5.24	6.64	5.97	6.71
Condenser	116.2	114.1	109.6	109.2
Generator	45.3	46.1	46.4	47.1

CONCLUSIONS

Thermal backup systems and plants or some energy storage systems are essential, when a considerable amount of wind power is injected into the grid. The findings of other studies showed energy costs of the wind with backup thermal, the wind with battery energy storage, and Wind Powered Thermal Energy System (WTES), which employs inductive heat generators and thermal energy storage systems, are comparable. Also, the results of this study show that the energy and exergy performance of the WTES system is also comparable with conventional wind and other energy storage systems. The results of the 2E analysis show that the exergy efficiency of the system is 28.9%, which is more than solar thermal system exergy efficiency. WTES becomes much more attractive when constructed besides CSP and/or bio-mass plants since many elements can be shared. The configuration of WTES has many variations. Employment of the electric and heat generator enables flexible operation. It can even absorb surplus energy from the grid. Employment of the superconducting heat generator realizes high working temperature, *i.e.*, high thermal to electric conversion efficiency. Those variations, including simple thermal specialized types, have lots of room to be investigated.

Data Availability Statement

The data that support the findings of this study are available from the corresponding author upon reasonable request.

Nomenclature			
Turbine	Turbine fluid	h	Specific enthalpy (kJ/kgK)
C	condenser	EX	Exergy flow, (kW or W)
m	Mechanical	m	Mass flow rate (kg/s or kg/h)
cold	Cold stream	N	Molar flow (mol/s)
HX	Exchanger	R	Universal gas constant (kJ/kgK)
in	inlet	Tm	melting point temperature, ℃
out	outlet	To	environment temperature, ℃
G	Heat generator	Ti	inner temperature, ℃
p	pump	EXpcm.i	exergy supplied to the PCM during charging, kW
ref	Working fluid		
t	turbine	EXpcm.o	exergy output from the PCM during discharging, kW
P	Pressure (kPa)		
q	Specific heat(kJ/kg)		
Q	Heat rate (kW)		
s	Specific entropy (kJ/kgK)		
T_0	Ambient temperature (K)		
η	Efficiency (%)		
$E_{product}$	Power to the grid (kW)		
mean	average		

REFERENCES

[1]   Gupta, D. K., Kumar, R., and Kumar, N. (2020). Performance analysis of PTC field based ejector organic Rankine cycle integrated with a triple pressure level vapor absorption system (EORTPAS). *Engineering Science and Technology, an International Journal*, 23(1), 82-91. DOI: https://doi.org/10.1016/j.jestch.2019.04.008

[2]   Kerme, E. D., Orfi, J., Fung, A. S., Salilih, E. M., Khan, S. U.-D., Alshehri, H., Ali, E., and Alrasheed, M. (2020). Energetic and exergetic performance analysis of a solar driven power, desalination and cooling poly-generation system. *Energy*, 196, 117150. DOI: https://doi.org/10.1016/j.energy.2020.117150

[3]   Alirahmi, S. M., Rahmani Dabbagh, S., Ahmadi, P., and Wongwises, S. (2020). Multi-objective design optimization of a multi-generation energy system based on geothermal and solar energy. *Energy Conversion and Management*, 205, 112426. DOI: https://doi.org/10.1016/j.enconman.2019.112426

[4]   Alotaibi, S., Alotaibi, F., and Ibrahim, O. M. (2020). Solar-assisted steam power plant retrofitted with regenerative system using Parabolic Trough Solar Collectors. *Energy Reports*, 6, 124-133. DOI: https://doi.org/10.1016/j.egyr.2019.12.019

[5]   Ehyaei, M. A., Ahmadi, A., El Haj Assad, M., and Salameh, T. (2019). Optimization of parabolic through collector (PTC) with multi objective swarm optimization (MOPSO) and energy, exergy and economic analyses. *Journal of Cleaner Production*, 234, 285-296. DOI: https://doi.org/10.1016/j.jclepro.2019.06.210.

[6]   Toghyani, S., Afshari, E., Baniasadi, E., and Shadloo, M. S. (2019). Energy and exergy analyses of a nanofluid based solar cooling and hydrogen production combined system. *Renewable Energy*, 141, 1013-1025. DOI: https://doi.org/10.1016/j.renene.2019.04.073

[7]   AlZahrani, A. A., and Dincer, I. (2018). Energy and exergy analyses of a parabolic trough solar power plant using carbon dioxide power cycle. *Energy Conversion and Management*, 158, 476-488. DOI: https://doi.org/10.1016/j.enconman.2017.12.071

[8]   Yilmaz, F. (2019). Energy, exergy and economic analyses of a novel hybrid ocean thermal energy conversion system for clean power production. *Energy Conversion and Management*, 196, 557-566. DOI: https://doi.org/10.1016/j.enconman.2019.06.028

[9]   Ishaq, H., and Dincer, I. (2020). Evaluation of a wind energy based system for co-generation of hydrogen and methanol production. *International Journal of Hydrogen Energy*, 45(32), 15869-15877. DOI: https://doi.org/10.1016/j.ijhydene.2020.01.037

[10]   Bamisile, O., Huang, Q., Li, J., Dagbasi, M., Desire Kemena, A., Abid, M., and Hu, W. (2020). Modelling and performance analysis of an innovative CPVT, wind and biogas integrated comprehensive energy system: An energy and exergy approach. *Energy Conversion and Management*, 209, 112611. DOI: https://doi.org/10.1016/j.enconman.2020.112611

[11]   Kianfard, H., Khalilarya, S., and Jafarmadar, S. (2018). Exergy and exergoeconomic evaluation of hydrogen and distilled water production via combination of PEM electrolyzer, RO desalination unit and geothermal driven dual fluid ORC. *Energy Conversion and Management*, 177, 339-349. DOI: https://doi.org/10.1016/j.enconman.2018.09.057

[12]   Alirahmi, S. M., and Assareh, E. (2020). Energy, exergy, and exergoeconomics (3E) analysis and multi-objective optimization of a multi-generation energy system for day and night time power generation - Case study: Dezful city. *International Journal of Hydrogen Energy*, 45(56), 31555-31573. DOI: https://doi.org/10.1016/j.ijhydene.2020.08.160

[13]   Mohammadi, K., Khaledi, M. S. E., Saghafifar, M., and Powell, K. (2020). Hybrid systems based on gas turbine combined cycle for trigeneration of power, cooling, and freshwater: A comparative techno-economic assessment. *Sustainable Energy Technologies and Assessments*, 37, 100632. DOI: https://doi.org/10.1016/j.seta.2020.100632

[14]   Okazaki, T., Shirai, Y., and Nakamura, T. (2015). Concept study of wind power utilizing direct thermal energy conversion and thermal energy storage. *Renewable Energy*, 83, 332-338. DOI: https://doi.org/10.1016/j.renene.2015.04.027

[15]   Razmi, A. R., and Janbaz, M. (2020). Exergoeconomic assessment with reliability consideration of a green cogeneration system based on compressed air energy storage (CAES). *Energy Conversion and Management*, 204, 112320. DOI: https://doi.org/10.1016/j.enconman.2019.112320

[16]   Rashidi, H., and Khorshidi, J. (2018). Exergoeconomic analysis and optimization of a solar based multigeneration system using multiobjective differential evolution algorithm. *Journal of Cleaner Production*, 170, 978-990. DOI: https://doi.org/10.1016/j.jclepro.2017.09.201

[17]   Nemati, A., Sadeghi, M., and Yari, M. (2017). Exergoeconomic analysis and multi-objective optimization of a marine engine waste heat driven RO desalination system integrated with an organic Rankine cycle using zeotropic working fluid. *Desalination*, 422, 113-123. DOI: https://doi.org/10.1016/j.desal.2017.08.012

[18]   Naseri, A., Bidi, M., Ahmadi, M. H., and Saidur, R. (2017). Exergy analysis of a hydrogen and water production process by a solar-driven transcritical CO2 power cycle with Stirling engine. *Journal of Cleaner Production*, 158, 165-181. DOI: https://doi.org/10.1016/j.jclepro.2017.05.005

[19]   Norouzi, N. (2021). The Pahlev Reliability Index: A measurement for the resilience of power generation technologies versus climate change. *Nuclear Engineering and Technology*, 53(5), 1658-1663. DOI: https://doi.org/10.1016/j.net.2020.10.013

[20]   Khajehpour, H., Norouzi, N., Bashash Jafarabadi, Z., Valizadeh, G., & Hemmati, M. H. (2021). Energy, exergy, and exergoeconomic (3E) analysis of gas liquefaction and gas associated liquids recovery co-process based on the mixed fluid cascade refrigeration systems. *Iranian Journal of Chemistry and Chemical Engineering (IJCCE)*. 'Article in Press' DOI: 10.30492/ijcce.2021.141462.4442

[21]   Habibollahzade, A., Gholamian, E., Ahmadi, P., and Behzadi, A. (2018). Multi-criteria optimization of an integrated energy system with thermoelectric generator, parabolic trough solar collector and electrolysis for hydrogen production. *International Journal of Hydrogen Energy*, 43(31), 14140-14157. DOI: https://doi.org/10.1016/j.ijhydene.2018.05.143